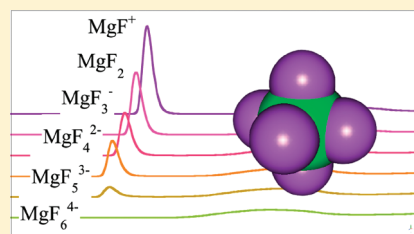


Theoretical Study of Magnesium Fluoride in Aqueous Solution

Naoto Shibata,[†] Hirofumi Sato,^{*,†} Shigeyoshi Sakaki,^{†,||} and Yuji Sugita^{‡,§}[†]Department of Molecular Engineering, Graduate School of Engineering, Kyoto University, Nishikyo-ku, Kyoto 615-8510, Japan[‡]RIKEN Advanced Science Institute, 2-1 Hirosawa, Wako-shi, Saitama 351-0198, Japan[§]RIKEN Quantitative Biology Center and RIKEN Advanced Institute for Computational Science, 7-1-26 Minatojima-Minamimachi, Chuo-ku, Kobe, Hyogo 650-0047, Japan

ABSTRACT: A series of magnesium fluorides (MgF_n^{2-n}), multiply charged anions, in the gas phase and in aqueous solution were theoretically studied with a hybrid approach of quantum chemistry and statistical mechanics, called RISM-SCF-SEDD theory. In the gas phase, MgF_3^- is the most stable species among the complexes ($n = 1-6$). In contrast, due to compensation between the intramolecular energy and solvation free energy, the stabilities of a number of complexes with different n are comparable in aqueous solution. Based on accurate evaluation of free energy change, the mole fraction of MgF_4^{2-} is the highest in the range from $\text{pF} = 2.0$ to 3.0 of aqueous solution. This is consistent with the available PDB data of the enzymes that catalyze the phosphoryl transfer reactions. The hydration structures of magnesium fluorides obtained by RISM-SCF-SEDD theory provide insight into their structural changes from the gas phase to aqueous solution.



INTRODUCTION

It is well recognized that a series of metal fluorides inhibits the phosphoryl transfer reaction in enzymes.¹⁻³ Aluminum fluoride and beryllium fluoride are widely utilized as phosphate analogues to provide structural information on the transition state of the reaction. While the mechanism of the reaction using these compounds draws great attention, the characteristics of metal fluorides themselves are still veiled in mystery. In particular, study on the state of magnesium fluoride (MgF_n^{2-n}) in aqueous solution is extremely limited. In the crystal structure, magnesium is found to be coordinated with 3 to 4 fluoride atoms, but it is not clear yet how many fluoride anions coordinate to the magnesium in the most stable magnesium fluoride complex in aqueous solution and how the complex changes the state depending on the environment.

From a different standpoint, the metal fluorides belong to the classification of multiply charged anions (MCAs), which play an important role in chemistry, material science, and biochemistry. Interestingly, while MCAs are ubiquitous in solution phase, they are usually unstable as an isolated species and scarcely observed because of the strong intramolecular Coulombic repulsion among the excess charges. In other words, they are present as stable entities inside protein or in solution phase due to the electrostatic field from the surroundings. The solvation from the microscopic point of view is essential to understand the stability and the functions of these interesting species. However, the computational study on magnesium fluorides has been very limited, and only a study based on the dielectric continuum model by Stefanovich et al. in 1998⁴ is known to the best of our knowledge.

In the present study, the RISM-SCF-SEDD method^{5,6} was used to study the series of magnesium fluorides in aqueous solution. In RISM (reference interaction site model) theory,

solvation is treated using an analytical description based on statistical mechanics of solvent molecules, which enables us to evaluate the free energy and solvation structure using a much smaller calculation amount compared to molecular simulation methods such as molecular dynamics. RISM-SCF-SEDD is a hybrid theory of RISM and the ab initio molecular orbital method and has been successfully applied to a variety of chemical phenomena including chemical reactions, chemical equilibrium, etc.⁷ Because the free energy change associated with Mg–F bond formation or dissociation in solution phase is essential to understand the stability of the complex, QM/MM or its alternative such as RISM-SCF-SEDD are a possible choice to properly describe the equilibrium. The dependence of fluoride concentration, which governs the state of the complex in reality, was also considered.

METHODS

Definition of Relative Energy. The following process and its free energy change in the gas phase (an isolated complex) as well as in aqueous solution are the focus of the present study



where n is the number of fluoride anions bound to a magnesium. In the gas phase, the free energy of the complex, MgF_n^{2-n} , is defined as the sum of the total energy associated with the electronic structure calculation ($E_{\text{gas}}^{\text{tot,cmplx}}(n)$) and the kinetic contribution that is readily calculated from the elementary statistical mechanics for ideal gas, i.e., translational, rotational,

Received: June 8, 2011

Revised: July 27, 2011

Published: August 17, 2011

and vibrational terms ($G_{\text{gas}}^{\text{kin,cmplx}}(n)$). To obey the mass conservation, the contribution from the unbound $(6 - n)$ fluoride anions ($G_{\text{gas}}^{\text{F anion}}$) in the system is also added.

$$\begin{aligned} G_{\text{gas}}(n) &= E_{\text{gas}}^{\text{tot,cmplx}}(n) + G_{\text{gas}}^{\text{kin,cmplx}}(n) + (6 - n)G_{\text{gas}}^{\text{F anion}} \\ &= E_{\text{gas}}^{\text{tot,cmplx}}(n) + G_{\text{gas}}^{\text{kin,cmplx}}(n) \\ &\quad + (6 - n)\{E_{\text{gas}}^{\text{tot,F anion}} + G_{\text{gas}}^{\text{kin,F anion}}\} \\ &= E_{\text{gas}}^{\text{tot}}(n) + G_{\text{gas}}^{\text{kin}}(n) \end{aligned} \quad (2)$$

where $E_{\text{gas}}^{\text{tot}}(n)$ is the sum of total energy of the complex and unbound F^- in the system.

$$E_{\text{gas}}^{\text{tot}}(n) = E_{\text{gas}}^{\text{tot,cmplx}}(n) + (6 - n)E_{\text{gas}}^{\text{tot,F anion}} \quad (3)$$

$G_{\text{gas}}^{\text{kin}}(n)$ is the kinetic contribution defined in a similar manner. For the sake of convenience, the difference from the standard value ($n = 0$) was introduced

$$\Delta G_{\text{gas}}(n) = G_{\text{gas}}(n) - G_{\text{gas}}(0) = \Delta E_{\text{gas}}^{\text{tot}}(n) + \Delta G_{\text{gas}}^{\text{kin}}(n) \quad (4)$$

$G_{\text{gas}}(0)$ corresponds to a state in which the magnesium and six fluoride ions are separately present in vacuo.

$$\begin{aligned} G_{\text{gas}}(0) &= G_{\text{gas}}^{\text{MG cation}} + 6G_{\text{gas}}^{\text{F anion}} \\ &\equiv E_{\text{gas}}^{\text{tot,cmplx}}(0) + G_{\text{gas}}^{\text{kin,cmplx}}(0) + 6G_{\text{gas}}^{\text{F anion}} \end{aligned} \quad (5)$$

In the aqueous solution phase, the infinitely diluted system is considered within the framework of RISM-SCF theory. The free energy of the solution system (G_{sol}) is given by

$$\begin{aligned} G_{\text{sol}}(n) &= E_{\text{sol}}^{\text{tot}}(n) + \delta\mu(n) + G_{\text{sol}}^{\text{kin}}(n) \\ &= E_{\text{gas}}^{\text{tot}}(n) + E^{\text{reorg}}(n) + \delta\mu(n) + G_{\text{sol}}^{\text{kin}}(n) \end{aligned} \quad (6)$$

The reorganization energy E^{reorg} is defined as $E_{\text{sol}}^{\text{tot}} - E_{\text{gas}}^{\text{tot}}$ corresponding to the energy needed to alter the electronic structure and molecular geometry upon transferring from the gas phase to the solution phase. The kinetic contributions in aqueous solution ($G_{\text{sol}}^{\text{kin}}$) is computed utilizing the correction of free volume theory proposed by Mammen et al.⁸ $\delta\mu$ is the sum of solvation free energies of the complex and separated anions. In the present treatment, an analytical expression is known for each species ($\delta\mu^{\text{X}}$; $\text{X} = \text{cmplx}, \text{F anion}$).

$$\delta\mu(n) = \delta\mu^{\text{cmplx}}(n) + (6 - n)\delta\mu^{\text{F anion}} \quad (7)$$

$$\delta\mu^{\text{X}} = \frac{\rho}{\beta} \sum_{\alpha}^{\text{X}} \sum_{\gamma} \int_0^{\infty} \left\{ \frac{1}{2} h_{\alpha\gamma}(r)^2 - 2c_{\alpha\gamma}(r) - h_{\alpha\gamma}(r)c_{\alpha\gamma}(r) \right\} 4\pi r^2 \text{d}r \quad (8)$$

where $h_{\alpha\gamma}(r)$ and $c_{\alpha\gamma}(r)$ are respectively the total and direct correlation functions between site α constituting X and solvent site γ . $\beta = 1/k_{\text{B}}T$, where k_{B} and T are the Boltzmann constant and temperature and ρ is number density of solvent. The relative value with respect to the standard value ($n = 0$) is similarly defined as follows:

$$\Delta G_{\text{sol}}(n) = \Delta E_{\text{gas}}^{\text{tot}}(n) + \Delta E^{\text{reorg}}(n) + \Delta\delta\mu(n) + \Delta G_{\text{sol}}^{\text{kin}}(n) \quad (9)$$

COMPUTATIONAL DETAILS

The new-generation of RISM-SCF (RISM-SCF-SEDD), in which the spatial electron density distribution (SEDD) was directly treated,⁵ was employed. Compared to the original version of RISM-SCF,⁹ the present version is free from grid dependency in the charge fitting procedure. Note the computation of MCA is not possible without the RISM-SCF-SEDD method because such a highly charged molecule often causes difficulties in the convergence of RISM procedure. Furthermore, the analytical energy gradient technique⁶ is also essential to properly compute an optimized molecular structure in aqueous solution.

All geometries were optimized using density functional theory (B3LYP) followed by energy calculations using CCSD(T) with cc-pVDZ basis set. Stefanovich et al.⁴ reported that this functional (B3LYP) provided very similar results with MP2 for this system. The Lennard-Jones parameters of the solute were taken from the literature^{10,11} ($\sigma_{\text{Mg}} = 1.644 \text{ \AA}$, $\sigma_{\text{F}} = 2.720 \text{ \AA}$, $\epsilon_{\text{Mg}} = 0.875 \text{ kcal/mol}$, $\epsilon_{\text{F}} = 0.348 \text{ kcal/mol}$) and SPC-like water was assumed for the solvent¹² ($\sigma_{\text{O}} = 3.166 \text{ \AA}$, $\sigma_{\text{H}} = 1.000 \text{ \AA}$, $\epsilon_{\text{O}} = 0.155 \text{ kcal/mol}$, $\epsilon_{\text{H}} = 0.056 \text{ kcal/mol}$). The solvent water density was set to 1 g/cm^3 at $T = 298.15 \text{ K}$. The RISM equation was solved with HNC closure.

The calculations in vacuo and in aqueous solution were carried out by Gaussian 03 and GAMESS packages. The latter was modified by us to perform the RISM-SCF-SEDD method.

RESULTS AND DISCUSSION

Molecular Geometry. The optimized geometry of the magnesium fluoride complex in vacuo is shown in Figure 1a. In each structure, Mg–F bonds are weakened and lengthened as the number of coordinating fluorine increased. All fluorides tend to keep away each other to reduce strong F–F Coulombic repulsion, and the bond angle is thus understandable in terms of the VSEPR model.

The solvent effect due to surrounding water molecules greatly affects the optimized geometry. The large geometry change was found in MgF_2 , MgF_3^- , MgF_4^{2-} , and MgF_5^{3-} where their bond angles were significantly bent as shown in Figure 1b. The Mg–F bonds in MgF_2 , MgF_3^- , and MgF_4^{2-} were evidently lengthened, whereas those in MgF_5^{3-} and MgF_6^{4-} were shortened. Stefanovich et al.⁴ reported the optimized geometries for MgF_3^- , MgF_4^{2-} , MgF_5^{3-} , and MgF_6^{4-} in aqueous solution using the dielectric continuum model. Their reported trends in bond lengths are almost similar with ours except for MgF_4^{2-} , but changing angles; that is, the symmetry breaking in the point group is essentially different from their report. Not only the solvent-effect treatment but also the basis set employed are different, and the former may be a crucial factor to determine the geometry of the system. As we will mention latter, strong hydrogen bonds are formed between the complex and surrounding water molecules. Note that a spherical Coulombic field generated by the magnesium cation plays a dominant role in determining the structure since Mg–F is regarded as a virtually pure ionic bond. It is very likely that the F–Mg–F bond angle is flexible enough and readily affected by the environment. The vacant site newly prepared by changing the F–Mg–F angle will be occupied by solvent water molecule. Actually, the energy curve at the equilibrium geometry is very flat, and the lowest frequency modes of MgF_4^{2-} in the gas phase are scissoring and

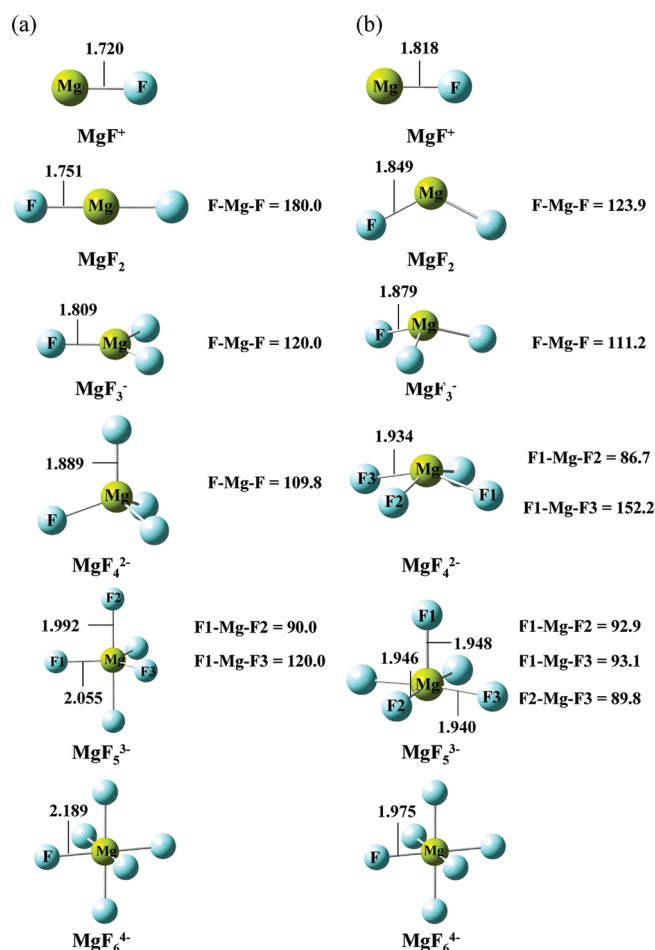


Figure 1. Optimized geometry of MgF_n^{2-n} ($n = 1 - 6$) in the gas phase (a) and in aqueous solution (b). Angles and bond lengths are given by degree and Å.

twisting around 150 cm^{-1} . A recent RISM-SCF-SEDD study by Viwat et al.¹³ may be related to the present issue. The computation demonstrates a symmetry breaking of NO_3^- in aqueous solution, which is perfectly consistent with experimental result of vibrational spectra, similar to the case of I_3^- in solution phase.¹⁴

Finally, the geometry of the phosphate analogues is also discussed. Much geometrical information of MgF_3^- and MgF_4^{2-} occluded by enzymes are available in the Protein Data Bank (PDB). The averaged Mg–F bond lengths and F–Mg–F angles for $n = 3^{15-17}$ are respectively $1.845 \pm 0.04\text{ Å}$ and $119.9 \pm 0.1^\circ$, intermediate values between the gas phase and aqueous solution. Similarly, the average values of $n = 4^{2,18-22}$ in crystal structures are $1.880 \pm 0.15\text{ Å}$ and $108.8 \pm 0.6^\circ$, which are much closer to the values in the gas phase. It may be related to the low dielectric condition of the protein inside. The loose bonding and flexible structure make it difficult to definitively conclude the structural status in solution phase.

Free Energy Change. The free energy changes in the gas phase ($\Delta G_{\text{gas}}(n)$) as well as in aqueous solution ($\Delta G_{\text{sol}}(n)$) are plotted in Figure 2a as a function of the number of fluoride atoms (n). It appears that both of the energy curves are respectively described as a quadratic function, and the obtained values in the gas phase are in good agreement with the previous report.⁴ The lowest free energy is found at $n = 3$ in the gas phase, whereas it is $n = 5$ in aqueous solution. The stability is governed by the

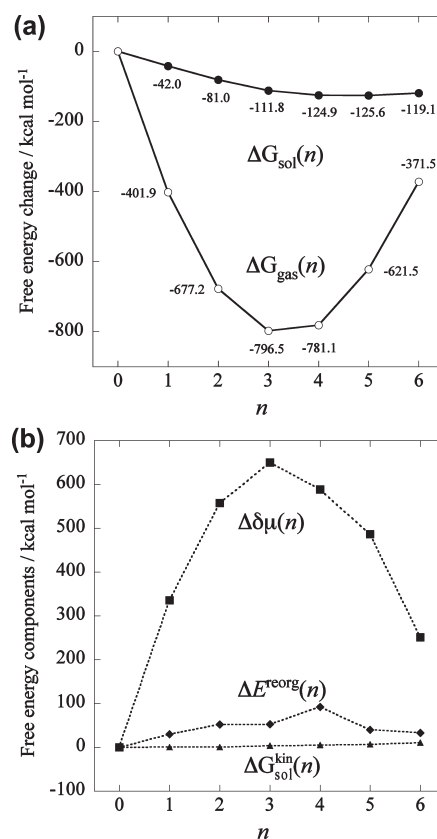


Figure 2. (a) Free energy change in the gas phase (open circles) and in aqueous solution (circles). (b) Energy components of $\Delta G_{\text{sol}}(n)$. Solvation energy ($\Delta\delta\mu$; squares), reorganization energy (ΔE^{reorg} ; diamonds), and kinetic term ($\Delta G_{\text{sol}}^{\text{kin}}$; triangles).

environment; MCAs with excess charges are stabilized by the electric field generated by solvent molecules. Compared to the gas phase system where the large n -dependency is observed, the curve in the aqueous solution phase shows modest change along the increasing of n .

The decomposed contributions to $\Delta G_{\text{sol}}(n)$ are displayed in Figure 2b. The difference from $\Delta G_{\text{gas}}(n)$ is mainly attributed to the large change in solvation free energy, which is given by

$$\Delta\delta\mu(n) = \delta\mu^{\text{cmplx}}(n) - \{\delta\mu^{\text{MG cation}} + n\delta\mu^{\text{F anion}}\} \quad (10)$$

Because $\delta\mu^{\text{MG cation}}$ and $\delta\mu^{\text{F anion}}$ are constant values, the contribution from the latter two terms in the curly parentheses depends on n linearly. The quadratic curvature of $\Delta\delta\mu(n)$ originates from the $\delta\mu^{\text{cmplx}}(n)$ term. Hence the free energy change in aqueous solution is essentially determined by the compensatory relation of the two contributions, $\Delta E_{\text{gas}}^{\text{tot}}(n)$ and $\Delta\delta\mu(n)$, especially $\delta\mu^{\text{cmplx}}(n)$ (see eq 9). $\Delta E^{\text{reorg}}(n)$ and $\Delta G_{\text{sol}}^{\text{kin}}(n)$ are also plotted in the figure, which look to be negligibly small compared to $\Delta\delta\mu$. However, these are also important to give the free energy, $\Delta G_{\text{sol}}(n)$, because of the subtle balance in the compensation between $\Delta E_{\text{gas}}^{\text{tot}}(n)$ and $\Delta\delta\mu(n)$.

Why are both of them quadratic functions and compensated each other? Since Mg–F bond is regarded as purely ionic and spherical atomic ions mainly participate the equilibrium in the present system, the mechanism is understood through a simple explanation as follows: The total energy may be simplified as the

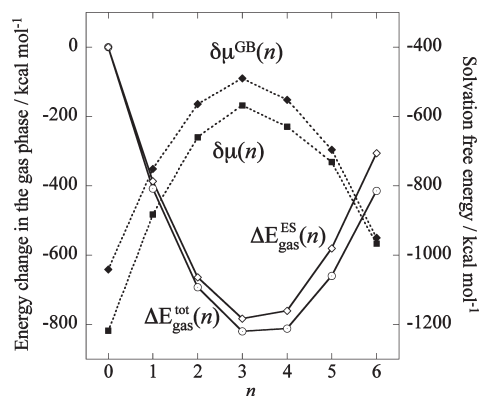


Figure 3. Energy change in the gas phase (left axis) and solvation free energy (right axis). The relative value, $\Delta E_{\text{gas}}^{\text{tot}} = E_{\text{gas}}^{\text{tot}}(n) - E_{\text{gas}}^{\text{tot}}(0)$, obtained by ab initio molecular orbital computations (circles) and $\Delta E_{\text{gas}}^{\text{ES}}(n)$ (open diamonds) are plotted with solid lines. Solvation free energy computed with RISM-SCF-SEDD, $\delta\mu(n)$ (squares), and $\delta\mu^{\text{GB}}(n)$ evaluated with generalized Born energy (diamonds) are plotted with dotted lines.

sum of electrostatic interactions among the magnesium cation and fluoride anions due to pure ionic nature of the bond.

$$E_{\text{gas}}^{\text{tot, cmplx}}(n) \approx E_{\text{gas}}^{\text{ES}}(n) = \sum_{i>j} \frac{q_i q_j}{r_{ij}} \quad (11)$$

where indices i and j run over the ion pairs, r_{ij} is the distance between them, $\text{Mg}-\text{F}$ and $\text{F}-\text{F}$. q_i is set to +2 and −1 for charge of magnesium and fluoride, respectively. $\Delta E_{\text{gas}}^{\text{ES}}(n)$ is plotted in Figure 3, together with the relative values of $\Delta E_{\text{gas}}^{\text{tot}}(n)$ obtained by the ab initio molecular orbital computation. Both of them are in reasonable agreement, and MgF_3^- is given as the lowest energy complex. Equation 11 can be further simplified if $r_{\text{Mg}-\text{F}}$ and $r_{\text{F}-\text{F}}$ are assumed to be constant values:

$$\begin{aligned} E_{\text{gas}}^{\text{ES}} &\approx \sum_i^{\text{F anion}} \frac{(+2) \times (-1)}{r_{\text{Mg}-\text{F}}} + \sum_{i>j}^{\text{F anion}} \frac{(-1)^2}{r_{\text{F}-\text{F}}} \\ &= \frac{-2n}{r_{\text{Mg}-\text{F}}} + \frac{n(n-1)}{2r_{\text{F}-\text{F}}} \end{aligned} \quad (12)$$

Apparently, the first term ($\text{Mg}-\text{F}$) shows a linear dependence on n , whereas the second term ($\text{F}-\text{F}$) is a quadratic function of n . By differentiating the above equation with respect to n , the minimum $n_{\text{min}} = 2r_{\text{F}-\text{F}}/r_{\text{Mg}-\text{F}} + 0.5$ is approximately estimated between 3 and 4, depending on the ratio of bond lengths. In essence, the Coulombic interaction is responsible for the changes of the total energy (intramolecular energy) displayed in the figure.

The solvation energy may be roughly estimated with dielectric continuum model although strong hydrogen bonding is formed in the present system as we will see later. The standard generalized Born (GB) theory for the solvation free energy proposed by Still et al.²⁴ was examined.

$$-\frac{1}{2} \left(1 - \frac{1}{\epsilon} \right) \sum_{i,j} \frac{q_i q_j}{f_{\text{GB}}} \quad (13)$$

where

$$f_{\text{GB}} = \sqrt{r_{ij}^2 + \alpha_i \alpha_j \exp \left(-\frac{r_{ij}^2}{4\alpha_i \alpha_j} \right)}$$

ϵ is the dielectric constant, α_i is the effective atomic radius of site i , and the standard effective radii was used for fluorine ($\alpha_{\text{F}} = 1.532 \text{ \AA}$).²⁴ Because the radii for magnesium was not available, the Lennard-Jones parameter was borrowed. As the sum of the contributions from the complex and independent n fluoride anions, total solvation free energy in this approximated treatment is given by

$$\delta\mu^{\text{GB}}(n) = -\frac{1}{2} \left(1 - \frac{1}{\epsilon} \right) \sum_{i,j} \frac{q_i q_j}{f_{\text{GB}}} - \frac{6-n}{2} \left(1 - \frac{1}{\epsilon} \right) \frac{1}{\alpha_{\text{F}}} \quad (14)$$

The obtained energy $\delta\mu^{\text{GB}}(n)$ and $\Delta\delta\mu(n)$ from RISM-SCF-SEDD are also plotted in Figure 3. GB results are reasonably close to RISM-SCF-SEDD values, although $\delta\mu^{\text{GB}}(n)$ systematically overestimates in smaller n region. This is because the dominant contributions in the region are attributed to the independently solvated fluoride anion. Although the solvation free energies of the complexes are not significantly different each other, a discrepancy between the two models is the largest in the evaluation for the fluoride anion, which is related to the hydrogen bond around F^- . Similar to the argument for $\Delta E_{\text{gas}}^{\text{ES}}(n)$, the quadric dependency of n is attributed to the first term in eq 14. Therefore, the physicochemical background of the complex formation and its solvation are respectively explained in a qualitative sense by the aid of two simple models. However, the most stable complex in terms of n is determined by the subtle balance between them. A quantitative evaluation based on statistical mechanics and highly accurate quantum chemical methods is necessary to correctly understand the phenomenon. Note that the present discussion about the energetics remains essentially the same even if the structural differences described in the previous section are considered.

Distribution Curves. The stability of the complex is affected by the concentration of ions in reality. Hence, the mole fraction is determined by the complex formation constant $K_{f,n}$:

$$K_{f,n} = \exp \left(-\frac{\Delta\Delta G_{f,n}}{RT} \right) = \frac{[\text{MgF}_n^{2-n}]}{[\text{MgF}_{n-1}^{3-n}][\text{F}^-]} \quad (15)$$

where R is gas constant and $\Delta\Delta G_{f,n}$ is defined as the free energy difference between complexes with different fluorination state in aqueous solution corresponding to eq 1.

$$\Delta\Delta G_{f,n} = \Delta G_{\text{sol}}(n-1) - \Delta G_{\text{sol}}(n) \quad (16)$$

The mole fraction α_n related to MgF_n^{2-n} is defined as

$$\begin{aligned} \alpha_n &= \frac{[\text{MgF}_n^{2-n}]}{[\text{Mg}^{2+}] + \sum_{m=1}^6 [\text{MgF}_m^{2-m}]} \\ &= \frac{K_{f,n} K_{f,n-1} \cdots K_{f,1} [\text{F}^-]^n}{1 + \sum_{m=1}^6 K_{f,m} K_{f,m-1} \cdots K_{f,1} [\text{F}^-]^m} \end{aligned} \quad (17)$$

where $K_{f,n}$ in eq 15 is substituted to give the final equation. By setting the concentration of fluoride, $\text{pF} = -\log[\text{F}^-]$, α_n is obtained using the computed free energy difference, $\Delta G_{\text{sol}}(n)$. Figure 4 plots α_n as a function of pF . α_n exhibits remarkable dependency, and the dominant complex is sequentially changed from MgF_5^{3-} to Mg^{2+} as pF increases. From experimental studies, magnesium fluoride complexes of $n = 3$ or 4 occluded by enzyme were obtained in the range of $\text{pF} = 2.0$ to 3.0.^{1,2,3}

The present computed fraction shows that MgF_4^{2-} is the dominant complex in such a condition with little fraction of MgF_5^{3-} , which is consistent with the available PDB data.

Solvation Structure. In RISM theory, solvation structure is expressed by a set of radial distribution functions (RDFs). Figure 5a depicts a set of RDFs between hydrogen (H) of solvent water and fluoride atom in the complex. The sharp peaks found in 1.6 Å are assigned as the hydrogen bond. Because the fluoride is exposed to solvent in all of the complexes, the peak positions are not changed at all. It is interesting that the peaks become higher and sharper up to MgF_4^{2-} and then become lower as n increases. The Mulliken charge on the fluoride reaches a minimum value (-0.797) at $n = 4$, which should be related to this behavior.

The RDFs between oxygen (O) and magnesium are shown in Figure 5b. The first peaks around 2.1 Å correspond directly to the

contacting solvent water molecule. As the number of bound fluorine atoms is increased, this conspicuous peak is gradually lowered and virtually disappeared for MgF_6^{4-} because the vacant site is not left due to the full coordination. It is also important that increasing the total negative charge tends to prohibit oxygen (water molecule) from approaching. The behavior may be related to six coordination of Mg^{2+} in aqueous solution and to the coordination of aluminum fluoride reported by Bodor et al.^{25,26} Another interesting point is that the second peak around 4.0 Å does not change with respect to n . It implies that the electric field generated by the central magnesium is not so different among all of the complexes. Presumably, the magnesium is always fully surrounded by fluorine anions or by water molecules, and the effect of their shielding is relatively independent of the fluorination state.

To confirm this point, the running coordinated number of water to solute magnesium was calculated.

$$N_{\text{Mg-O}}(r) = \rho \int_0^r dr 4\pi r'^2 g_{\text{Mg-O}}(r') \quad (18)$$

where ρ is the number density of water. $N_{\text{Mg-O}}(r)$ is plotted in Figure 6. The functions rise at 2 Å in all of the complexes except for MgF_6^{4-} , which starts beyond 3 Å. For $n = 5$ (MgF_5^{3-}), the function is almost constant ($N_{\text{Mg-O}}(r) \approx 1$) in a range between $r = 2$ and 3 Å, indicating that one water molecule is directly attached to the complex. In other words, the magnesium is surrounded by six moieties consisting of five fluoride ligands and one water molecule. A similar explanation is applicable to other complexes, although the coordination number is slightly overcounted, in particular for the larger n complex. The contributions beyond 3 Å correspond to the second hydration as mentioned above.

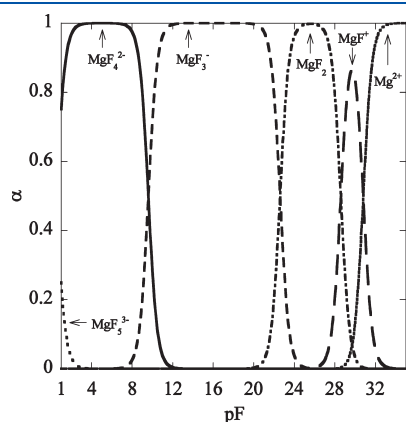


Figure 4. pF dependence of the mole fraction of MgF_n^{2-n} (α_n).

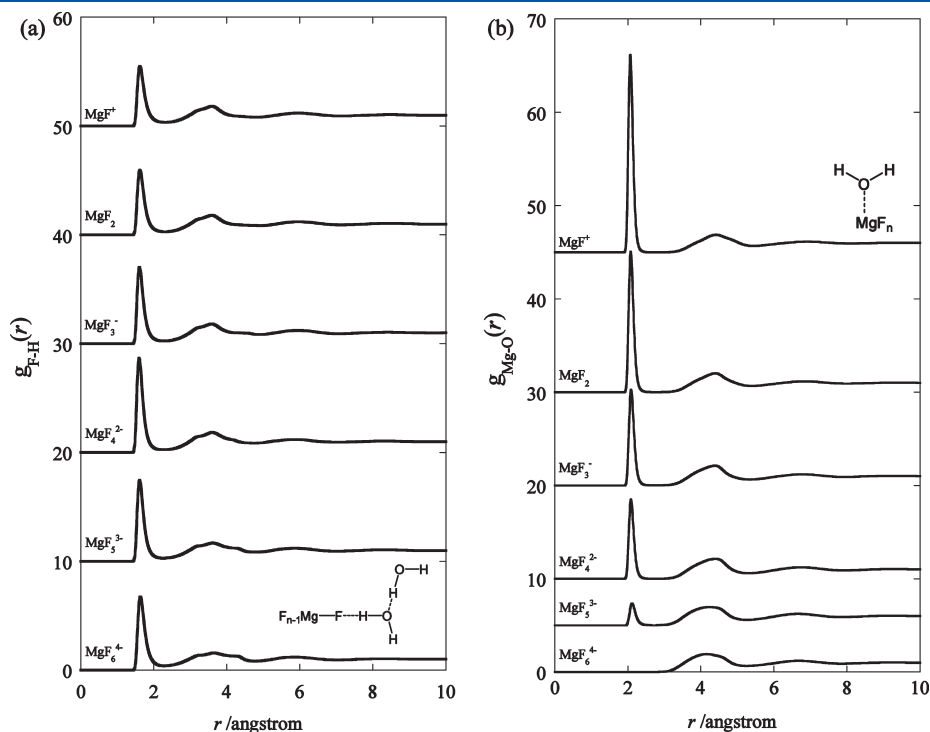


Figure 5. (a) RDF of solvent hydrogen around F atom and (b) RDF of solvent oxygen around Mg atom.

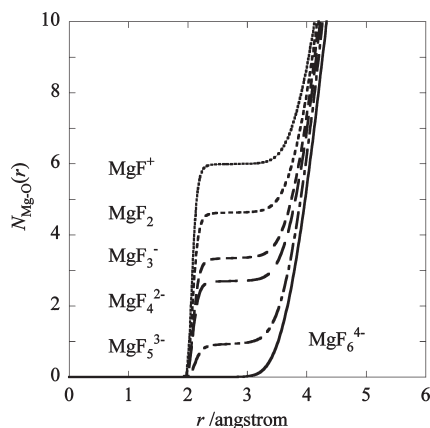


Figure 6. Running coordination number for radial distribution function between magnesium and water oxygen.

CONCLUSIONS

The stability of magnesium fluoride, a multiply charged anion, in the gas phase and in aqueous solution was theoretically studied with a hybrid approach of quantum chemistry and statistical mechanics, called RISM-SCF-SEDD theory. Based on accurate evaluation of free energy change as a function of the coordination number n , the mole fraction of the complex in aqueous solution was calculated. It was found that MgF_4^{2-} is the dominant complex in experimental conditions, which may be consistent with the fact that the enzymes that occlude magnesium fluoride might react with MgF_4^{2-} .

Utilizing two simple models, it was shown that the stability of the complex is governed by two factors. One is the intramolecular interaction within a complex, which may be understood through Coulombic interactions between $\text{Mg}-\text{F}$ and $\text{F}-\text{F}$. The other is the intermolecular interaction between the complex and the solvent. However, the consequent stability of the complex is determined by a subtle balance between them, and accurate evaluation of the free energy is necessary. In this sense, careful consideration on the solvation free energy including hydrogen-bonding effect is indispensable to adequately understand the phenomenon.

As mentioned in the Introduction, metal fluorides, including magnesium fluoride, aluminum fluoride, and beryllium fluoride, are widely utilized as phosphate analogues to inhibit the phosphoryl transfer reactions in enzymes. Interestingly, the gas-phase geometries of MgF_3^- and MgF_4^{2-} are found to be much similar to those in the enzyme structures. Considering the nearly equal stability in free energy, MgF_3^- and MgF_4^{2-} appear to be flexible in solution and change their geometries into those in low dielectric conditions like the gas phase or inside the protein. Another important point might be that replacement of metal in the fluorides is able to capture different reaction intermediates of the phosphoryl transfer reactions in enzymes. Accurate evaluation of Coulombic interactions and the careful consideration of the solvation free energy should be indispensable to understand such biochemical phenomena.

AUTHOR INFORMATION

Corresponding Author

*E-mail: hirofumi@moleng.kyoto-u.ac.jp.

Present Addresses

^{||} Fukui Institute for Fundamental Chemistry, Kyoto University, Takano-Nishihiraki-cho, 34-4, Sakyo-ku, Kyoto 606-8103, Japan.

ACKNOWLEDGMENT

The authors gratefully acknowledge the valuable comments and suggestions made by Mr. Kentaro Kido. The work is financially supported in part by a Grant-in-Aid for Scientific Research on Priority Areas "Molecular Science for Supra Functional Systems" (477-22018016), a Grant-in-Aid for Scientific Research on Innovative Areas "Molecular Science of Fluctuations" (2006-21107511, 23107714), as well as a Grant-in-Aid for Scientific Research (C) (20550013). All of them were supported by the Ministry of Education, Culture, Sports, Science and Technology (MEXT) Japan.

REFERENCES

- (1) Graham, D. L.; Lowe, P. N.; Grime, G. W.; Marsh, M.; Rittinger, K.; Smerdon, S. J.; Gamblin, S. J.; Eccleston, J. F. *Chem. Biol.* **2002**, *9*, 375.
- (2) Toyoshima, C.; Nomura, H.; Tsuda, T. *Nature* **2004**, *432*, 361.
- (3) Bigay, J.; Deterre, P.; Pfister, C.; Chabre, M. *J. EMBO* **1987**, *6*, 2907.
- (4) Stefanovich, E. V.; Boldyrev, A. I.; Truong, T. N.; Simon, J. *J. Phys. Chem. B* **1998**, *102*, 4205.
- (5) Yokogawa, D.; Sato, H.; Sakaki, S. *J. Chem. Phys.* **2007**, *126*, 244504.
- (6) Yokogawa, D.; Sato, H.; Sakaki, S. *J. Chem. Phys.* **2009**, *131*, 214504.
- (7) (a) Iida, K.; Yokogawa, D.; Sato, H.; Sakaki, S. *Chem. Phys. Lett.* **2007**, *443*, 264. (b) Iida, K.; Yokogawa, D.; Ikeda, A.; Sato, H.; Sakaki, S. *Phys. Chem. Chem. Phys.* **2010**, *11*, 8556. (c) Hayaki, S.; Yokogawa, D.; Sato, H.; Sakaki, S. *Chem. Phys. Lett.* **2008**, *458*, 329. (d) Sato, H.; Kikumori, C.; Sakaki, S. *Phys. Chem. Chem. Phys.* **2011**, *13*, 309. (e) Higashi, M.; Kato, S. *J. Phys. Chem. A* **2005**, *109*, 9867. (f) Hayaki, S.; Kido, K.; Sato, H.; Sakaki, S. *Phys. Chem. Chem. Phys.* **2010**, *12*, 1822. (g) Hayaki, S.; Kido, K.; Yokogawa, D.; Sato, H.; Sakaki, S. *J. Phys. Chem. B* **2009**, *113*, 8227.
- (8) Mammen, M.; Shakhnovich, E. I.; Deutch, J. M.; Whitesides, G. M. *J. Org. Chem.* **1998**, *63*, 3821.
- (9) Ten-no, S.; Hirata, F.; Kato, S. *J. Chem. Phys.* **1994**, *100*, 7443. Sato, H.; Hirata, F.; Kato, S. *J. Chem. Phys.* **1996**, *105*, 1546.
- (10) Aqvist, J. *J. Phys. Chem.* **1990**, *94*, 8021.
- (11) Yoshida, N.; Phongphanphane, S.; Maruyama, Y.; Imai, T.; Hirata, F. *J. Am. Chem. Soc.* **2006**, *128*, 12042.
- (12) Berendsen, H. J. C.; Postma, J. P. M.; van Gunsteren, W. F. *J. Comput. Chem.* **1986**, *7*, 230.
- (13) Vchirawongkwin, V.; Sato, H.; Sakaki, S. *J. Phys. Chem. B* **2010**, *114*, 10513.
- (14) Sato, H.; Hirata, F.; Myers, A. B. *J. Phys. Chem. A* **1998**, *102*, 2065.
- (15) Baxter, N. J.; Bowler, M. W.; Alizadeh, T.; Cliff, M. J.; Hounslow, A. M.; Wu, B.; Berkowitz, D. B.; Williams, N. H.; Blackburn, G. M.; Waltho, J. P. *Proc. Natl. Acad. Sci. U.S.A.* **2010**, *107*, 4555.
- (16) Lee, J. Y.; Yang, W. *Cell* **2006**, *127*, 1349.
- (17) Wouters, J.; Oudjama, Y.; Stalon, V.; Droogmans, L.; Poulter, C. D. *Proteins* **2004**, *54*, 216.
- (18) Shinoda, T.; Ogawa, H.; Cornelius, F.; Toyoshima, C. *Nature* **2009**, *459*, 446.
- (19) Ogawa, H.; Shinoda, T.; Cornelius, F.; Toyoshima, C. *Proc. Natl. Acad. Sci. U.S.A.* **2009**, *106*, 13742.
- (20) Laursen, M.; Bublit, M.; Moncoq, K.; Olesen, C.; Moeller, J. V.; Young, H. S.; Nissen, P.; Morth, J. P. *J. Biol. Chem.* **2009**, *284*, 13513.
- (21) Morth, J. P.; Pedersen, B. P.; Toustrup-Jensen, M. S.; Sorensen, T. L.; Petersen, J.; Andersen, J. P.; Vilsen, B.; Nissen, P. *Nature* **2007**, *450*, 1043.
- (22) Moncoq, K.; Trieber, C. A.; Young, H. S. *J. Biol. Chem.* **2007**, *282*, 9748.

- (23) Baxter, N. J.; Blackburn, G. M.; Marston, J. P.; Hounslow, A. M.; Cliff, M. J.; Bernal, W.; Williams, N. H.; Hollfelder, F.; Wemmer, D. E.; Waltho, J. P. *J. Am. Chem. Soc.* **2008**, *130*, 3952.
- (24) Still, W. C.; Tempczyk, A.; Hawley, R. C.; Hendrickson, T. *J. Am. Chem. Soc.* **1990**, *112*, 6127.
- (25) Kim, H.-S. *J. Mol. Struct. (THEOCHEM)* **2001**, *541*, 59.
- (26) Bodor, A.; Toth, I.; Banyai, I.; Szabo, Z.; Hefter, G. T. *Inorg. Chem.* **2000**, *39*, 2530.